Development of Large Area Photon Counting Detectors Optimized for Cherenkov Light Imaging with High Temporal and sub-mm Spatial Resolution

O.H.W. Siegmund, *Member, IEEE*, J.B. McPhate, S.R. Jelinsky, J.V. Vallerga, A.S. Tremsin, *Member, IEEE,* R. Hemphill, H.J. Frisch, R.G. Wagner, J. Elam, A. Mane and the LAPPD Collaboration

***Abstract*–Progress towards the development of a 20 cm sealed tube optical detector with imaging and photon event time stamping is presented. Novel microchannel plates employing borosilicate micro-capillary arrays have been tested. These provide many performance characteristics typical of conventional MCPs, but have been made in sizes up to 20 cm, have low intrinsic background (0.085 events cm^{-2} s^{-1}) and very stable gain behavior for at least 1 C cm^{-2} of charge extraction. Bialkali (Na_2KSb) photocathodes with > 20% quantum efficiency have also been made on borofloat-33 windows compatible with a 20 cm sealed tube device.**

I. Introduction

The development of large area imaging and timing detectors with high performance has advantages for many potential applications, but also presents some significant challenges. For example, in the application of detection of Cherenkov light in neutrino detection, timing resolution of a few picoseconds and spatial resolution of <1 mm over areas of 20 cm would be advantageous. Currently available devices are limited to sizes of about 5 cm and use either conventional microchannel plates (MCPs), or dynode multipliers for amplification, coupled to pad array readouts. Extension of these schemes to devices as large as 20 cm presents significant problems and potentially considerable cost. A collaboration (Large Area Picosecond Photon Detector, LAPPD) [1] of the University of Chicago, Argonne National Laboratory, University of California, Berkeley, and a number of other national laboratories, universities and commercial companies have undertaken the task of employing novel technologies to develop a 20 cm format sealed tube visible sensitive detector.

The operational scheme of the photodetector is illustrated in Fig. 1. Incoming light passes through an entrance window (Borofloat 33) and interacts with a semitransparent photocathode on the inside of the window. The photoelectrons produced cross a proximity gap and are detected by an MCP pair. This pair of novel borosilicate substrate MCPs, that are functionalized by atomic layer deposition, amplify the signal and the resulting electron cloud is detected by a strip line anode for determination of event positions and time of arrival.

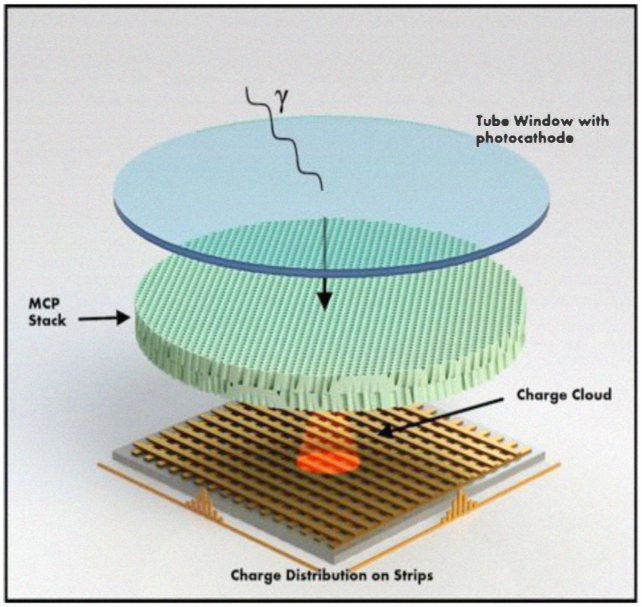

Fig. 1. Depiction of a sealed tube microchannel plate detector. Incoming photons pass through an entrance window and are converted to photoelectrons by a semitransparent photocathode. A microchannel plate stack multiplies the photoelectron and the resulting charge is collected by a strip-line anode.

Development of such a device in a 20 cm format presents some unique challenges: hermetic sealing to a large entrance window, a 20 cm semitransparent photocathode with good efficiency and uniformity, 20 cm MCPs with reasonable cost and performance, robust construction to preserve high vacuum and withstand an atmosphere pressure differential. The development plan at University of California, Berkeley is based on a conventional kovar/ceramic brazed assembly,

Manuscript received November 22, 2011. This work was supported in part by the U.S. Department of Energy under contract DE-AC02-06CH11357.

O. H. W. Siegmund is with the University of California, Berkeley, CA 94720 USA (telephone: 510-642-0895, e-mail: ossy@ssl.berkeley.edu).

J. B. McPhate is with the University of California, Berkeley, CA 94720 USA (telephone: 510-643-8242, e-mail: mcphate@ssl.berkeley.edu).

S. R. Jelinsky is with the University of California, Berkeley, CA 94720 USA (telephone: 510-643-7893, e-mail: sharonj@ssl.berkeley.edu).

J. V. Vallerga is with the University of California, Berkeley, CA 94720 USA (telephone: 510-6432-5666, e-mail: jvv@ssl.berkeley.edu).

A. S. Tremsin is with the University of California, Berkeley, CA 94720 USA (telephone: 510-642-4554, e-mail: ast@ssl.berkeley.edu).

R. Hemphill is with the University of California, Berkeley, CA 94720 USA (telephone: 510-642-6208, e-mail: rhemp@ssl.berkeley.edu).

H. J. Frisch is with the University of Chicago, Chicago, IL 94720 USA (telephone: 773-702-7479, e-mail: frisch@hep.uchicago.edu).

R. G. Wagner is with the Argonne National Lab. Lemont, IL 94720 USA (telephone: 630-252-6321, e-mail: rgwcdf@hep.anl.gov).

J. Elam is with the Argonne National Lab. Lemont, IL 94720 USA (telephone: 630-252-3520, e-mail: jelam@anl.gov).

A. Mane is with the Argonne National Lab. Lemont, IL 94720 USA (telephone: 630-252-1342, e-mail: amane@anl.gov).

The LAPPD collaboration is based at the Argonne National Lab. Lemont, IL 94720 USA (telephone: 630-252-6321, web: http://psec.uchicago.edu/).

while Argonne Laboratory is developing a lower-cost all-glass device. The sealed tube concept for the Berkeley effort is shown in Fig. 2. A stripline array anode on an Al_2O_3 substrate with contact pins for each stripline is brazed to an Al_2O_3 frame with a kovar indium well that facilitates the hot sealing of a Borofloat 33 entrance window. The MCPs are spaced, and held in place by ceramic "X's" that accommodate the stress distribution for an atmosphere pressure differential. High voltage contacts are made with pin feedthroughs, and getters are installed to help maintain the high vacuum in the enclosure. The chosen photocathode is a bialkali as this provides reasonable sensitivity in the region of interest and provides low background event rate and high stability. The MCPs are based on a novel concept where the substrate is constructed from a borosilicate (700°C softening point) micro-capillary array that is made to function as an MCP by deposition of resistive and secondary emissive layers using atomic layer deposition (ALD) [2, 3]. This differs from conventional MCP lead glass construction [4], removing the need for chemical etching and H_2 reduction steps, allowing the operational parameters to be set by tailoring the sequential ALD deposition processes. The process is relatively inexpensive compared with conventional MCPs and allows very large MCPs to be produced with pore sizes in the 40 µm to 10 µm range.

Each of the critical elements of the detector system has been evaluated to establish its performance characteristics and assess compatibility for a 20 cm sealed tube detector. In the case of the borosilicate ALD MCPs, considerable development and optimization has been done to achieve devices that are able to accommodate the 20 cm format.

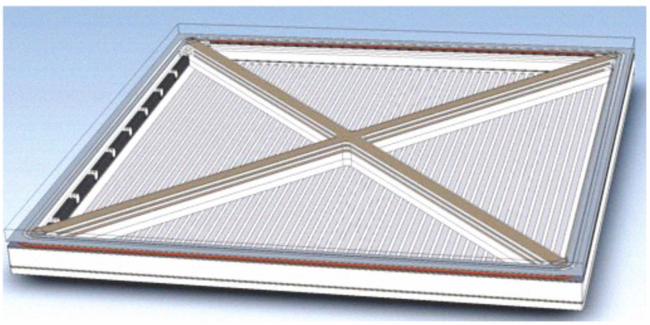

Fig. 2. Structure of a 20 cm "flat panel" microchannel plate sealed tube detector. A large borofloat-33 entrance window is indium sealed to a brazed ceramic-Kovar body that has a strip-line anode readout. The microchannel plates (not shown) are clamped between "X" spacers to accommodate an atmosphere pressure differential. Getters are used to maintain high vacuum.

II. Alkali Photocathodes

The deposition of large area photocathodes has been established for photomultipliers for some time. However, the implementation of large area photocathodes for sealed tube transfer photocathodes, which are required for this program, is not a well established process. The largest commercially available devices with transfer photocathodes are of the order 50 mm. After considering issues affecting the implementation of alkali photocathodes for 20 cm MCP based proximity focused sealed tubes we have selected Na_2KSb bialkali photocathode as a viable starting material. This photocathode material has a low background rate, and low resistivity, with a high temperature tolerance compared with other bialkali photocathode types [5]. However its quantum efficiency is not as high as K_2CsSb photocathodes, and there is no information about its behavior with our chosen Borofloat 33 window substrate. Therefore we have initiated an evaluation of Na_2KSb bialkali photocathodes deposited on Borofloat 33 windows.

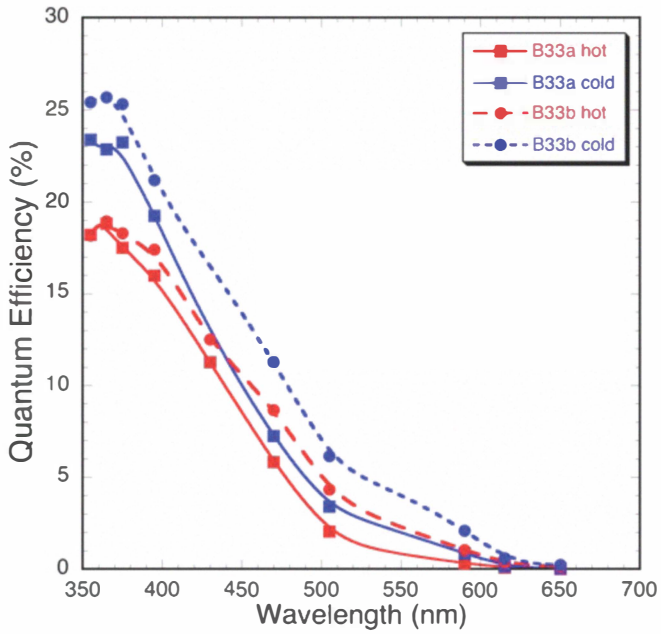

Fig. 3. Quantum efficiency for two depositions of Na_2KSb cathodes on Borofloat 33 31 mm windows measured immediately after deposition (hot) and a day later (cold) show good efficiency for these bialkalis on borosilicate.

Initial tests have been made by simultaneously depositing Na_2KSb semitransparent photocathodes onto four 31 mm diameter Borofloat 33 window substrates arranged within a 75 mm square area. The photocathode quantum efficiency as a function of wavelength was measured in comparison with a standard photodiode immediately after the photocathodes were completed (hot) and at ambient temperature (Fig. 3). Two separate photocathode deposition processes are shown in Fig. 3. In each case the photocathode quantum efficiency as a function of wavelength improved after the cathode had cooled. This result is encouraging in that it supports the requirement that window transfer and seal can be done without compromising the photocathode. No changes in the photocathode quantum efficiencies were seen over the week following deposition while the photocathode remained at high vacuum. The wavelength dependence of the quantum efficiency is typical of Na_2KSb semitransparent photocathodes, and the quantum efficiency values achieved are comparatively high. The tests also verify the compatibility of Borofloat 33 as a good window substrate. Our next verification tests will attempt to deposit Na_2KSb semitransparent photocathodes on 20 cm Borofloat 33

windows so that the overall photocathode uniformity over large areas can be assessed and optimized.

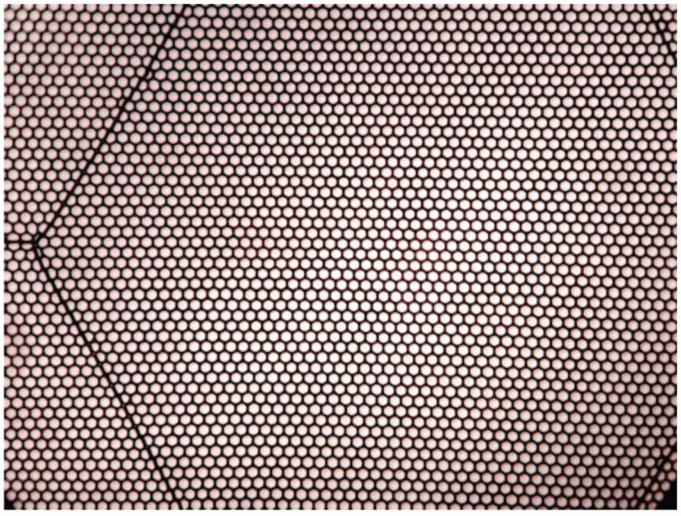

Fig. 4. Photograph of a 20 µm pore microchannel plate borosilicate substrate having 65% open area. Pore sizes are uniform except for the row adjacent to the multifiber boundary, which are distorted.

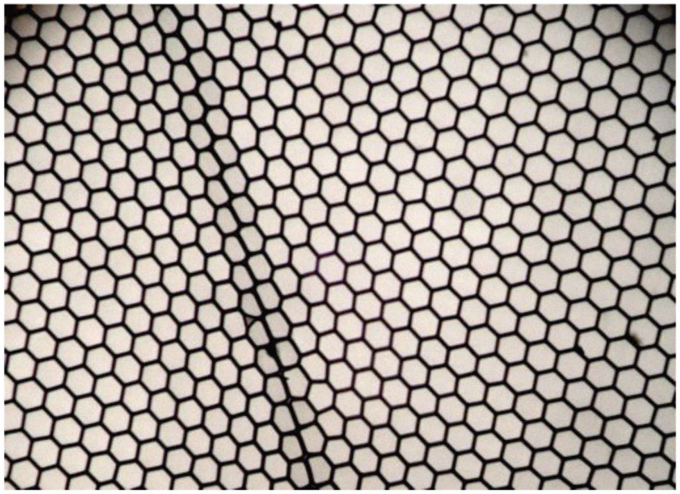

Fig. 5. Photograph of a 40 µm pore borosilicate microchannel plate having 83% open area. Several rows of pores adjacent to the multifiber boundary are distorted, but the large open area increases detection efficiency.

III. Borosilicate Microchannel Plates

Borosilicate micro-capillary array substrates functionalized with ALD layers to produce working MCPs require all the performance parameter optimizations customarily needed for a conventional MCP. However, in this case we can largely separate the substrate optimization and resistive/emissive layer optimization since these are sequential operations. The substrate optimization includes issues of cleanliness and debris removal, but also involves minimization of pore crushing at the multifiber boundaries and keeping the pore sizes uniform over the entire substrate.

Initial substrates [6] showed pore size non-uniformity and multifiber boundary crushing that were significant, producing significant image modulation. More recent 20 µm and 40 µm pore, 33 mm substrates (Figs. 4, 5) produced by INCOM Inc. have much improved structure as seen by optical inspection. The ability to tailor the pore open area ratio, up to values of > 80% (Fig. 5) also has implications for the event detection efficiency. The pore uniformity is also very good for the much larger 20cm substrates (Fig. 6) indicating that even over large areas this substrate methodology is a viable option.

In concert with the substrate optimizations, several ALD chemistries have been examined for the resistive layer application. Additionally ALD coatings of Al_2O_3 and MgO have been evaluated as the secondary emissive layer. Details of the ALD processes are discussed in more detail elsewhere [2], but considerable progress has been made in duplicating, and in some cases exceeding, conventional MCP performance characteristics.

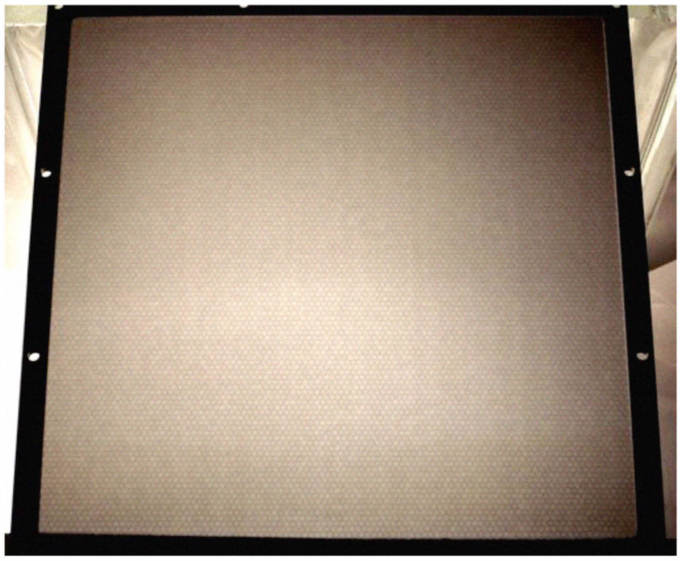

Fig. 6. Backlit photograph of a 20 cm MCP with 40 µm pores and 8° bias showing the uniformity of the multifiber stacking arrangement.

A. 33 mm Microchannel Plate Performance Characteristics

A significant part of the testing and optimization of the ALD borosilicate MCP development has been accomplished using 33 mm diameter MCPs. The nominal configuration has been 20 µm pore size, 60:1 pore L/d ratio and 8° pore bias angle. The majority of our evaluation tests were done in photon counting imaging detectors that employ a pair of MCPs and a cross delay line readout anode [7]. In this configuration there is a ~7 mm MCP output to anode gap, and the MCPs may be placed back to back, or spaced apart with a bias applied over the gap. Uniform illumination with 185 nm ultraviolet (UV) light is the typical excitation method. A number of MCPs have been tested to determine the critical performance behavior traits.

The first measurements to be done in each test are the gain as a function of applied voltage and the pulse amplitude distribution. Fig 7 shows a typical result for a pair of ALD borosilicate MCPs with a gap between the MCPs. The gain values can exceed 10^7 with a peaked (saturated) pulse height distribution. This is close to that expected for conventional MCPs [8, 9] with similar physical specifications. Images accumulated (Fig. 8) under 185 nm UV illumination show the

overall uniformity of response is good. However, the multifiber modulation of the top MCP, and faintly, the bottom MCP are both seen. A few small defects are seen close to the multifiber triple points. The image edge ring effect is due to field distortions related to the MCP mounting ring of the detector. An average gain image map taken at the same time shows the gain is uniform to better than 10% over the field of view. Additionally, the multifiber boundary zones have gain ~15% lower than other areas, presumably due to the local area crushing of pores.

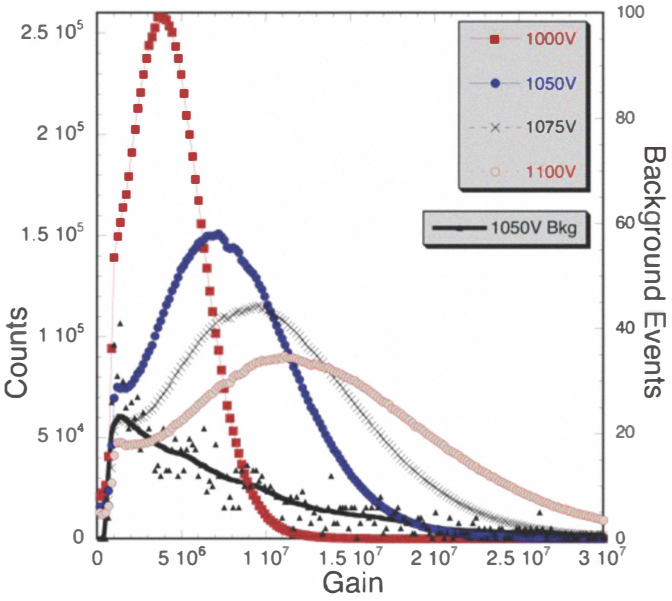

Fig. 7. Pulse height amplitude distributions for a 33 mm ALD borosilicate MCP pair. 20 µm pores, 8° bias, 60:1 L/d, 0.7 mm – 300V pair gap - bias, 185 nm illumination. 3000 sec background accumulation, 0.085 events cm^{-2} s^{-1}.

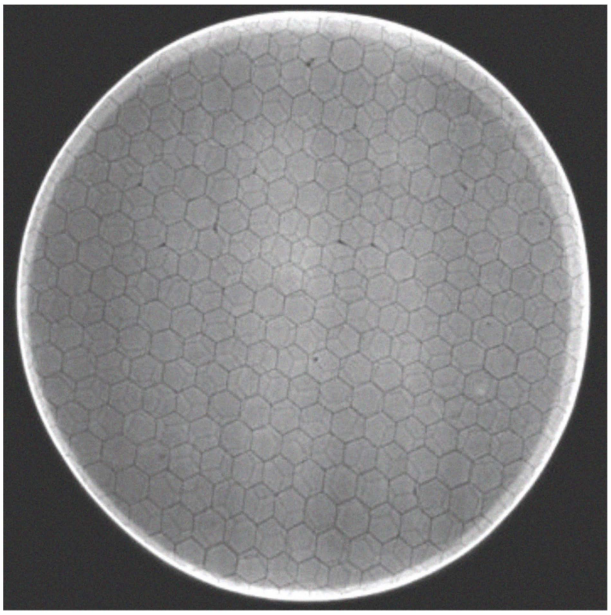

Fig. 8. Photon counting accumulated image using 185 nm illumination. ALD borosilicate MCP pair, 20 µm pore, 60:1 L/d, 8° bias, 0.7 mm/1000 V MCP pair gap/bias, at 7 x 10^6 gain, 1025 V bias on each MCP.

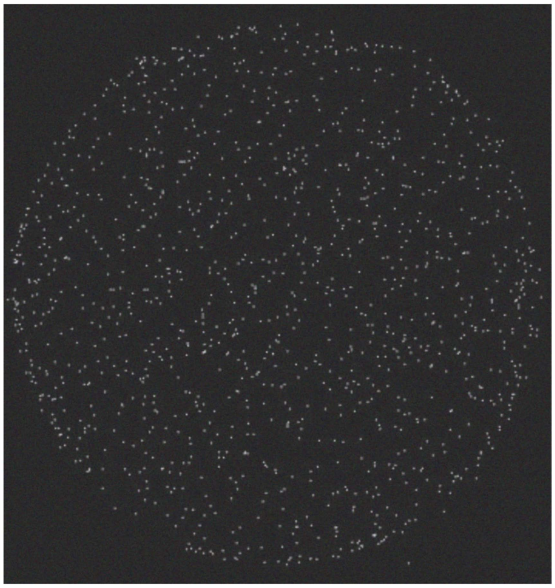

Fig. 9. Background event image. ALD borosilicate MCP pair, 20 µm pore, 60:1 L/d, 8° bias, 0.7 mm/1000 V MCP pair gap/bias, 3000 sec background, 0.087 events cm^{-2} s^{-1} at 7 x 10^6 gain, 1025 V bias on each MCP.

The spatial distribution of background events is found to be quite uniform. Furthermore, the negative exponential distribution of background events in Fig. 7 is indicative of a source of events that is evenly distributed throughout the MCP material. However, the observed rate of 0.085 events cm^{-2} s^{-1} is much less than conventional MCPs. This is the result of a considerable reduction in the amount of alkali (K, Rb) material in the MCP glass substrate, which dominates [9] the background rate for conventional MCPs.

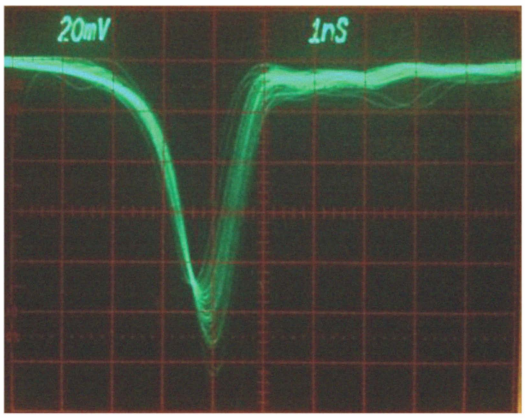

Fig. 10. Fast pulse response from single photons detected with an ALD borosilicate MCP pair, 20 µm pore, 60:1 L/d, 8° bias, 0.7 mm/1000 V MCP pair gap. Single event pulses are <1.25 ns wide.

The fast pulse response of single-photon amplified events was examined with a fast amplifier (150 ps risetime) and a 1 GHz analog oscilloscope. The event response of a 20 µm pore MCP pair is shown in Fig. 10 with the trigger amplitude set high to allow the pulse shape to be seen more clearly. The ~1.25 ns pulse width and pulse fall-time are comparable to conventional MCPs with the same geometry. Time tagging of these events to the accuracy of the MCP transit time jitter

should provide event timing resolution to much better than 100 ps.

B. GaN Opaque Photocathodes on Microchannel Plates

Applications of MCP detectors for UV (< 200 nm) sensing often use opaque photocathode layers [10] directly deposited onto the MCP surfaces to achieve the best quantum efficiency and imaging characteristics. This is normally not possible for optically sensitive photocathodes such as the bialkali and CsTe materials due to processing constraints and contamination by, and of, the MCPs. The ALD borosilicate MCPs offer a potentially cleaner, more robust (700°C softening point) and tolerant substrate for opaque photocathode materials. We have investigated this opportunity by depositing opaque GaN (p-doped) photocathode onto an ALD borosilicate MCP by molecular beam epitaxy [11]. The GaN deposition was done selectively so that several different thicknesses were deposited in 6 sections of the MCP (Fig. 12). One section was uncoated, exposing the MCP electrode material, while other sections had thicknesses from 100 nm up to 1000 nm. The typical p dopant concentration is of the order 10^{19}, and it is expected that the GaN penetration into the MCP pores is asymmetrical due to the pore bias angle. Since the deposition conditions were not optimal, and the effective substrate material was NiCr on the MCP, the surface lattice matching is poor producing a polycrystalline/amorphous GaN layer.

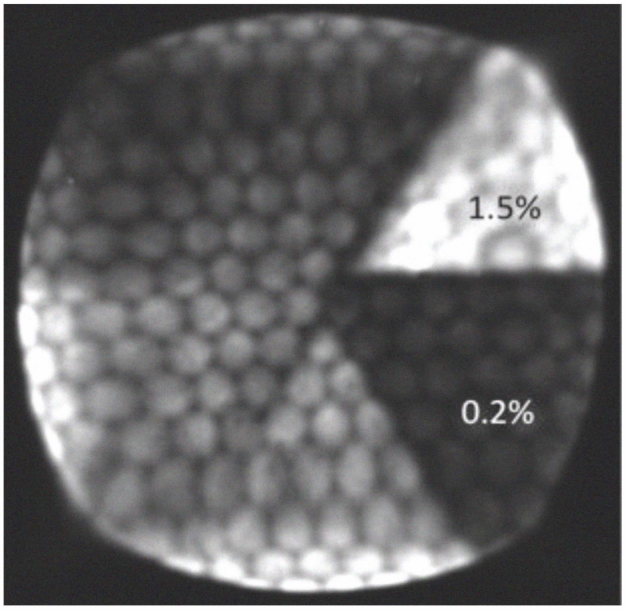

Fig. 11. Photon counting accumulated image using 185 nm (45°) illumination. ALD borosilicate MCP pair, 20 µm pore, 60:1 L/d, 8° bias, with GaN of deposited by MBE onto the top MCP (Fig. 12). Quantum efficiency measured for the bare MCP and 300 nm GaN zone are shown.

For testing of this photocathode we used the GaN coated MCP as the top MCP of a pair, installed into a detector with a cross delay line photon counting imaging readout. Measurement of the relative efficiency of the as deposited GaN in the MCP pores at an angle of ~45° (Fig. 11) shows a significant increase in quantum efficiency for the zone coated with 300 nm GaN. However, without Cs surface activation it is not possible to achieve optimal quantum efficiency performance. Therefore after a vacuum bake at ~300°C, Cs was deposited to reduce the surface work function. Measurements of the surface (MCP web area) quantum efficiency for 214 nm light were then taken at several incident angles (Fig. 12). In the opaque photocathode configuration the quantum efficiency increases as the photocathode layer increases until the layer fully attenuates the incoming radiation, or when the photoelectrons generated can no longer reach the emission surface. Thus the quantum efficiency tends to an asymptote value as the GaN layer thickness increases as is seen in Fig 12. Illumination at a 45° angle produces photoelectrons in the GaN closer to the emission surface (increasing the probability of transport to the surface and emission), thus the quantum efficiency values are significantly higher. The value of 17% is not as high as the 35% values achieved at the same wavelength for opaque GaN photocathodes on matched sapphire (Al_2O_3) substrates that we have measured previously [11]. However, it is significant that this level of efficiency has been achieved on a non-optimal substrate and without a Cs deposition optimization process. Al_2O_3 deposition is one of the standard ALD depositions used for the MCP fabrication process so further improvements may be possible by using ALD to deposit an Al_2O_3 film onto the top surface of the MCP prior to GaN deposition.

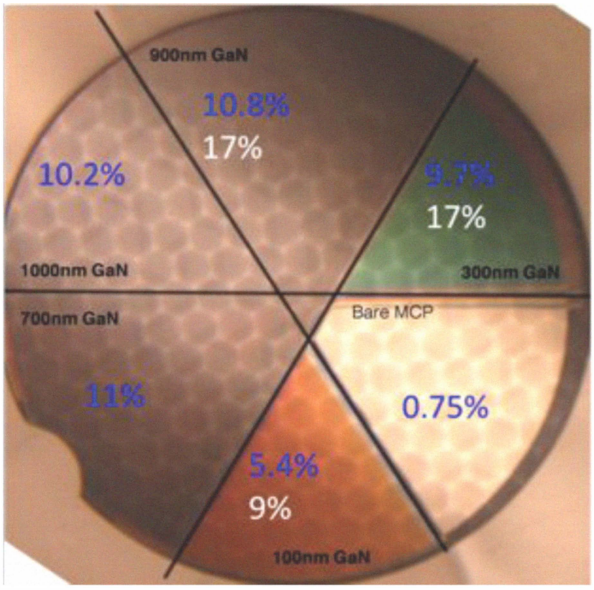

Fig. 12. ALD borosilicate MCP pair, 20 µm pore, 60:1 L/d, 8° bias, with GaN of several thicknesses deposited by MBE onto the top MCP. Quantum efficiency for the bare MCP and GaN zones are shown, measured after Cs deposition, 10° (blue) or 45° (white) angle to MCP normal (214 nm UV).

IV. MCP Preconditioning and Lifetime

Application of MCPs in sealed tube detectors incur a variety of issues. Amongst these are the evolution of gas from the MCPs and its effect on the lifetime of a sealed tube from the perspective of contamination effects, and of ion feedback damage to the photocathode. In most sealed tubes of this type precautions (preconditioning) are taken to reduce these effects,

including a vacuum bake and a charge extraction "burn in" or "scrub" to minimize the gas load and to stabilize the operation of the MCPs [12]. Further precautions are also taken in some cases [13], including a thin protective layer on top of the MCP top surface, or between two MCPs in a stack, to prevent ion feedback. Although these methods are effective in reducing ion feedback they also reduce the electron detection efficiency of the detector. Generally the MCP gain reduces as a function of extracted charge [12], however this is not usually the limiting factor on device lifetime as the gain can normally be re-established by applying higher MCP bias voltage. In conventional MCP operation a ~350°C vacuum bake followed by extraction of ~ 0.2 C cm^{-2} is adequate to reduce the gas evolution and stabilize the MCP gain [12].

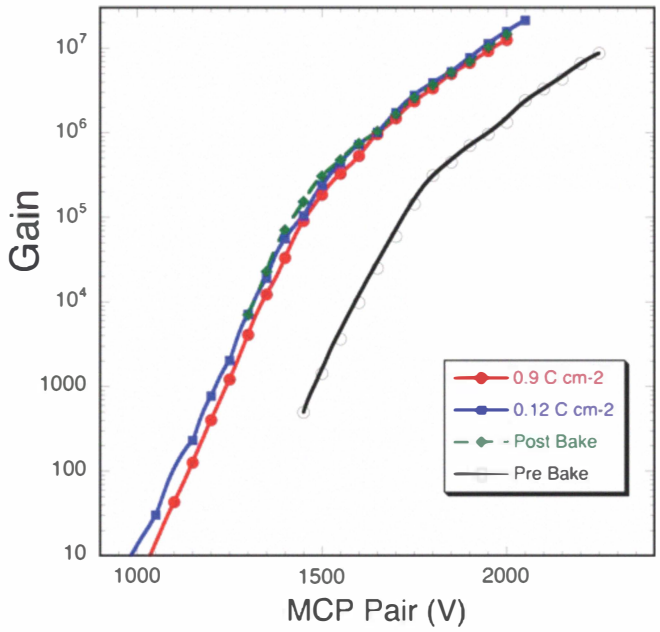

Fig. 13. Gain as a function of voltage for an ALD borosilicate MCP pair (20 µm pore, 60:1 L/d, 8° bias) at several stages of preconditioning operations. Significant gain increase was seen after the vacuum bake step.

We have begun the assessment of the vacuum bake and burn in characteristics of ALD borosilicate MCPs. A detector accommodating pairs of 33 mm MCPs using a cross delay line readout anode, and with all components implemented in metal or ceramic has been assembled for these tests. The first test of ALD MCP preconditioning (Fig. 14) using an early ALD formulation indicated that the gain of the ALD borosilicate MCPs (#613 & #612) did not change during the bake process. Subsequently the "burn-in" was very similar to that expected for conventional MCPs. The ALD materials and processes have been modified since that test, and so a second test with new MCPs was initiated. In this case a pair of MCPs (#163 & #164) was used, in a stack with a 25 µm thick unbiased gap between them. The MCP resistances were each ~150 MΩ with 20 µm pores, 60:1 L/d and 8° bias angle. Initially the gain and imaging characteristics were assessed in the same manner as described in section IIIA, with results similar to those presented in that section. The gain as a function of voltage characteristic is shown in Fig. 13. Prior to any pre-conditioning steps the gain reaches ~ 10^7 when 2250 V is applied to the pair, and the gain curve shows the onset of gain saturation at about 3 x 10^5 gain. After cooling following a high vacuum bake lasting ~ 40 hours and peaking at ~350°C the corresponding gain curve (Fig. 14) shows a gain increase of a factor of ~10 at applied MCP pair voltages above 1700 V, and increases of a factor of ~100 below 1600 V. Functional tests show no substantial differences in the imaging and background behavior, no differences in the uniformity of the gain across the field of view, and no changes in the uniformity of response to UV light. Residual gas analyzer data taken during the bake shows substantial reduction in the water vapor and atmospheric gases, as is expected for a typical vacuum bake operation. The substantial gain increase may occur as a result of surface cleaning of the ALD secondary emissive layer. Some secondary electron emissive materials do show increases in their emission coefficient with the removal of surface contaminants, and this would potentially result in higher MCP gain.

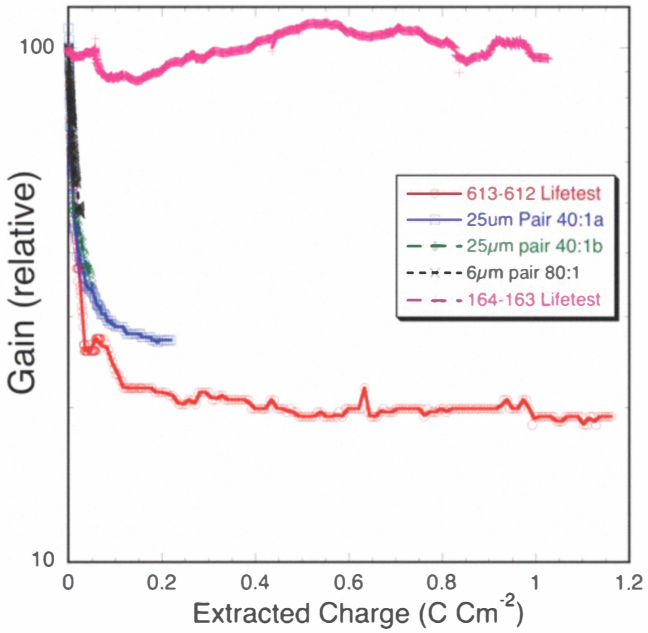

Fig. 14. Charge extraction for 33 mm ALD MCP pairs #613-613 and #164-163, (20µm pore, 60:1 L/d, 8° bias) compared with conventional MCPs. Typical charge extraction rates of 1 to 3 µA, at gain of ~10^5 using UV flood.

Following the vacuum bake, a "burn-in" of the MCPs was begun (Fig. 14). The configuration used a 185 nm UV full illumination as the input stimulation, and a gain of ~ 3 x 10^5 was established resulting in an output current of ~1 µA. Gas evolution was relatively low compared with conventional MCPs, with a differential pressure contribution of only a few x 10^{-10} torr attributable mainly to hydrogen evolution from the MCPs (as indicated by residual gas analysis performed continuously throughout the test). Adjusting the input UV flux, the output current was increased to ~2 µA when the extracted charge reached 0.05 C cm^{-2} and to ~3 µA when the extracted charge reached 0.12 C cm^{-2}. The applied voltage was never adjusted. Unlike the earlier ALD MCP "burn-in" test, and conventional MCP "burn-in" trends (Fig. 14), the gain

changes by only small amounts, without a precipitous initial drop. The apparent lack of substantial gas evolution and gain change infers a level of cleanliness and robustness of the ALD MCP surface layers that is not normally seen for conventional MCPs. Although these tests need to be repeated and verified, a significant MCP gain increase on vacuum bake, and an absence of significant gain change during charge extraction would have major consequences in many MCP applications.

V. 20 cm Borosilicate ALD MCP Tests

A small number of 20 cm square borosilicate substrate MCPs have been fully ALD functionalized to date, both in 40 µm and 20 µm pore sizes. We have been able to test a pair of these in a detector designed to perform photon counting imaging tests by employing a large cross delay line anode readout (Fig. 15). The MCPs are spring clamped around the periphery, and have a 0.7 mm insulating spacer between them that allows a bias to be applied to this inter-MCP gap. There is a 6 mm MCP to anode gap to allow the charge cloud to spread before impacting the anode. A cross delay line serpentine anode [14] with a 20 cm active area is used for the readout. The serpentine period is 4 mm with equal charge sharing between the upper and lower orthogonal serpentines. End to end delay times are ~100 ns to permit high overall event rate encoding and modest spatial resolution (~25 ps electronic time resolution).

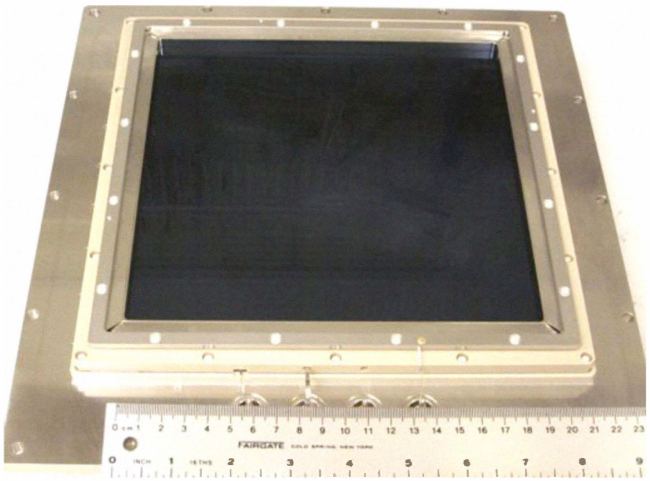

Fig. 15. 20 cm ALD 40 µm pore, 40:1 L/d, 8° bias MCP pair in a detector assembly with a cross delay line imaging readout for photon counting tests.

The initial 20 cm MCPs tested were a 40µm pore, 40:1 L/d, 8° bias MCP pair with resistances of 25 MΩ and 400 MΩ. A 400 V MCP gap bias was applied, and various MCP to anode bias settings were used to examine the anode encoding imaging performance. 185 nm UV light illuminated the entire detector at photon rates < 150 kHz. The highest average gain achieved was of the order 10^7 with individual MCP biases of ~ 1400 V. An image of the MCP pair response, which was obtained by accumulating ~ 5 x 10^8 events, is shown in Fig. 16. The striations in X and Y are modulations due to the anode period, indicating that the charge spreading on the anode is not optimal. An increase of the MCP-anode gap would improve this behavior. Some darker patches are seen around the edges of the image, which are areas of lower UV responsivity due to surface contaminants on the NiCr electrode material. This may be resolved with better handling/cleaning processes. A magnified inset shows the local area detail in one zone. The multifiber structure is clearly visible, as it is on the smaller 33 mm MCPs. Overall the average gain of the 20 cm MCP pair varies by up to a factor of three over the surface of the MCP.

The background event spatial distribution for this 20 cm MCP pair is shown in Fig. 17. The most obvious features are the patches and streaks of higher event rate. All of these were identified as events with high gain, which supports the identification of these as the result of field emission effects. This is most likely field emission from debris on the surface of the top MCP, which can be resolved by better handling and cleaning processes. Nevertheless the total background rate is ~0.24 events cm^{-2} s^{-1} for the integrated field of view, and only 0.075 events cm^{-2} s^{-1} for an area not displaying field emission effects (Fig. 17).

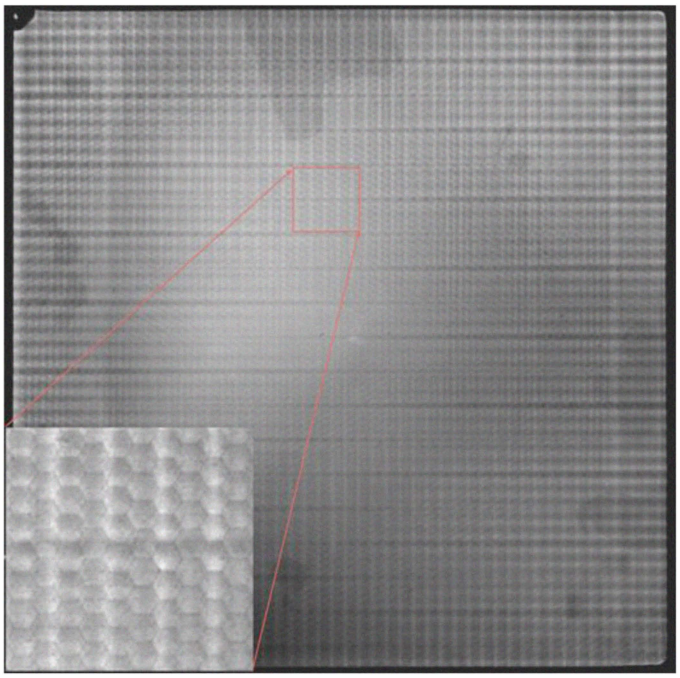

Fig. 16. Photon counting image (4096 x 4096 bins) accumulation for a 20 cm, 40 µm pore, 40:1 L/d ALD-MCP pair, 0.7mm pair gap/400v, using 185nm UV illumination. The overall striping in X and Y are due to the detector readout anode periodicity of 4 mm. The darker patches are variations in UV response for the MCP NiCr electrode. The inset shows an expanded 2 x 2 cm area revealing the imaging of multifiber structure of the MCPs.

The intrinsic background is comparable to the values seen on the 33 mm ALD borosilicate MCPs, and is considerably lower than conventional MCPs. For a 20 cm MCP this rate implies an overall background rate of < 50 events s^{-1}, which is far less than the background rate generated by a bialkali photocathode in a sealed tube device 20 cm in size. One other background feature not visible on the overall background image is the presence of several "warm spots" with relatively low event rate (< 1 event s^{-1}) in small localized areas. Two of

these can be seen in a 2cm x 2cm section of the background image as shown in Fig. 18a, and their spatial histograms are shown in Fig. 18b. The spatial histograms show that the spatial resolution of the detector system is at least 100 µm FWHM and indicates that the warm spots must be restricted to areas only a few MCP pores in size. The implications of these observations are that the detector system has at least 2 k x 2 k resolution elements, and that there is a small occurrence of debris in the MCP pores causing field emission.

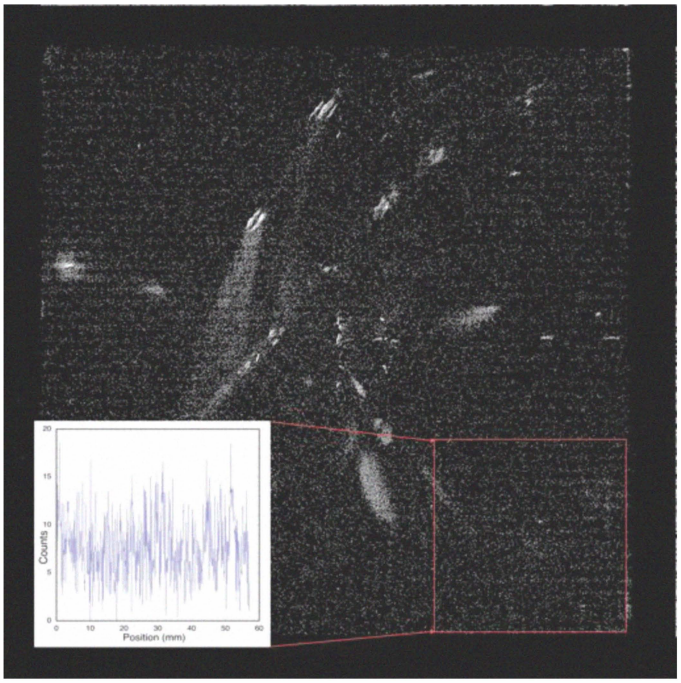

Fig. 17. Backround event image accumulation (2000 sec) for a 20 cm, 40 µm pore, 40:1 L/d ALD-MCP pair, 0.7mm pair gap/400v, gain ~5 x 10^6. Overall background 0.24 events cm^{-2} s^{-1} including the observed field emission and a few low rate "warm spots" resulting from debris on the MCPs. The inset shows an X histogram of the background events in a 6 x 6 cm area is quite uniform, and has a rate of 0.075 events cm^{-2} s^{-1}.

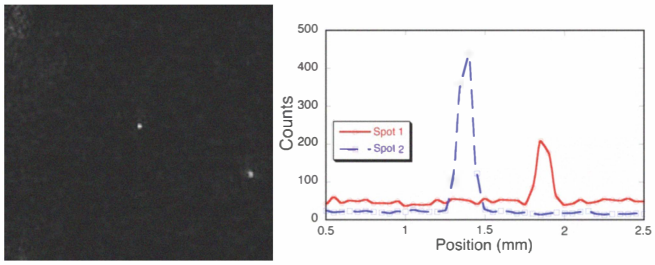

a) b)

Fig. 18. Imaging of "warm spots" for a 20 cm, 40 µm pore, 40:1 L/d ALD-MCP pair, 0.7mm pair gap/400v, gain ~5 x 10^6. a) image of two spots caused by debris in the MCP pores. b) X histograms of two spots showing that they are imaged with ~100 µm FWHM spatial resolution.

Despite the issues encountered with this first test of large area borosilicate MCPs it is significant that this initial test has produced a useful metric. In addition the MCPs were operated over periods of hours without issues. Relatively modest effort is required to suppress the anode modulation pattern, and with better cleanliness, eliminate the response variations. The gain variations are a result of the non-uniformity of the ALD layer coatings. Optimization of the large area ALD is underway and ALD tests have been done with 33 mm substrates distributed over a 20 x 20 cm area, which showed gain variations of ±10%. Thus, after some process adjustments it should be possible to resolve the current 20 cm MCP performance issues.

ACKNOWLEDGMENT

We wish to thank the members of the team at INCOM, Inc., Arradiance Inc., Dr. A. Dabiran at SVT associates, Mr. J. Hull, and Mr. J. Tedesco for their contributions to this work.

REFERENCES

[1] http://psec.uchicago.edu/
[2] Mane. A. 2011, "A novel atomic layer depostition method to fabricate economical and robust large area microchannel plates for photodetectors," Proceedings of Technology and Instrumentation in Particle Physics 2011, Physics Procedia, in press.
[3] M. Ritala and M. Leskelä. Nanotechnology, **10:1**, 19. (1999)
[4] M. Lampton, The microchannel image intensifier, Scientific American, **245**, 62-71, (1981).
[5] A. V. Lyashenko, A. Breskin, R. Chechik, J. M. F. Dos Santos, F. D. Amaro, J. F. C. A. Veloso, JINST 4 (2009) P07005
[6] O.H.W. Siegmund, J.B. McPhate, J.V. Vallerga, A.S. Tremsin, S.R. Jelinsky, H.J. Frisch, "Novel large format sealed tube microchannel plate detectors for Cherenkov timing and imaging", Nucl. Instr. Meth. **639(1)**, pp165-168, (2011)
[7] O. Siegmund, J. Vallerga, P. Jelinsky, X. Michalet, and S. Weiss, "Cross Delay Line Detectors for High Time Resolution Astronomical Polarimetry and Biological Fluorescence Imaging", Proc. IEEE Nuclear Science Symposium, ISBN: 0-7803-9222-1, pp. 448-452, (2005).
[8] J.L. Wisa, "Microchannel plate detectors", Nucl. Instr. Meth. **162** pp.587-601, (1979)
[9] O.H.W. Siegmund, Methods of vacuum ultraviolet physics, Chapter III, 2nd edition, ed's J.A.R. Samson and D.L. Ederer, Academic Press, (1998).
[10] O.H.W. Siegmund , B.Y. Welsh, J.V. Vallerga, A.S. Tremsin, J.B. McPhate, "High-performance microchannel plate imaging photon counters for spaceborne sensing", Proc. SPIE **6220**, (2006).
[11] O.H.W. Siegmund, Tremsin, Anton S., Vallerga, John V., McPhate, Jason B., Hull, Jeffrey S., Malloy, James, Dabiran, Amir M. "Gallium nitride photocathode development for imaging detectors" Proc. SPIE, **7021**, p.40, (2008)
[12] O.H.W. Siegmund, "Preconditioning of microchannel plate stacks," *Proc. SPIE*, **1072**, 111-118 (1989).
[13] Uhlig. F, Britting. A, Eyrich, W, and Lehmann. A. "Systematic Studies of Microchannel Plate PMTs", Nuclear Instruments and Methods Section A, in press 2011.
[14] O.H.W. Siegmund, J.V. Vallerga, B. Welsh, J. McPhate, A. Tremsin, "High speed optical imaging photon counting microchannel plate detectors for astronomical and space sensing applications", Proceedings of the Advanced Maui Optical and Space Surveillance Technologies Conference. p. 90. (2009)